Oxysterol	CAS #	MW
15-Ketocholestane	55823-04-6	402.65
15-Ketocholestene	50673-97-7	400.64
15α-hydroxycholestane	73389-49-8	404.67
15α-hydroxycholestene	26758-45-2	402.65
15ß-hydroxycholestene	26660-51-5	402.65
1α,25-dihydroxy vitamin D3	32222-06-3	416.64
1α-hydroxy vitamin D3	41294-56-8	400.64
22(R)-hydroxycholesterol	17954-98-2	402.65
22(S)-hydroxycholesterol	22348-64-7	402.65
24(R)-24,25-dihydroxy-vitamin D3	55721-11-4	416.64
24(R)-hydroxycholesterol	27460-26-0	402.65
24(S)-hydroxycholesterol	474-73-7	402.65
24(R/S),25-Epoxycholesterol	72542-49-5	400.64
24(S),25-Epoxycholesterol	77058-74-3	400.60
25-hydroxycholesterol	2140-46-7	402.65
27-hydroxycholesterol	20380-11-4	402.65
3ß-hydroxy-7-oxo-5-cholestenoic acid	1246298-64-5	430.62
3ß,7a-dihydroxy-5-cholestenoic acid	115538-84-6	432.63
3ß,7ß-dihydroxy-5-cholestenoic acid	1246298-66-7	432.64
4ß-hydroxycholesterol	17320-10-4	402.65
5-Cholesten-3β-ol-7-one	566-28-9	400.64
5α-Cholest-7-en-3β-ol	80-99-9	386.65
5α-Cholestan-3β-ol	80-97-7	388.67
5α-Cholestane	481-21-0	372.67
5α-Cholestan-3-one	566-88-1	386.65
5α,6α-Epoxycholestanol	1250-95-9	402.65
5β,6β-Epoxycholestanol	4025-59-6	402.65
5β-Cholestan-3α-ol	516-92-7	388.67
6-Ketocholestanol	1175-06-0	402.65
6α-hydroxy-5α-cholestanol	41083-73-2	404.67
7-Dehydrocholesterol	434-16-2	384.64
7-Ketocholesterol	566-28-9	400.64
7α,27-dihydroxycholesterol	4725-24-0	418.65
7α-hydroxycholesterol	566-26-7	402.65
7β,27-dihydroxycholesterol	240129-43-5	418.65
7β-hydroxycholesterol	566-27-8	402.65
7α,27-dihydroxy-4-cholesten-3-one	192187-67-0	416.64
7a,25-dihydroxycholesterol	64907-22-8	418.65

Oxysterol	CAS #	MW
7b,25-dihydroxycholesterol	64907-21-7	418.65
Cholecalciferol	67-97-0	384.64
Cholestenone	601-57-0	384.64
Cholesterol	57-88-5	386.65
15ß-hydroxycholestane	80656-42-4	404.67
7-keto-27-hydroxycholesterol	240129-30-0	416.64
7α-hydroxy-3-oxo-4-cholestenoic acid	1246298-65-6	430.62
5α,6ß-dihydroxycholestanol	1253-84-5	420.67
desmosterol	313-04-2	384.64
stigmasterol	83-48-7	412.69
lanosterol	79-63-0	426.72
24,25-dihydrolanosterol	911660-54-3	428.73
zymosterol	128-33-6	384.64
lathosterol	80-99-9	386.65
trihydroxycholestanoic acid	547-98-8	450.65
14-demethyl-lanosterol	7448-02-4	412.69
8(9)-dehydrocholesterol	70741-38-7	384.64
8(14)-dehydrocholesterol	177962-82-2	384.64
14-demethyl-14-dehydrolanosterol (FF-MAS)	64284-64-6	410.68
zymosterone	27192-37-6	382.62
3ß-hydroxy-5-cholestenoic acid	56845-87-5	416.64
3-oxo-4-cholestenoic acid	309762-85-4	414.62
27-hydroxy cholestenone	56792-59-7	400.64
diosgenin	512-04-9	414.62
Dehydroepiandrosterone sulfate (DHEA sulfate)	651-48-9	390.47
Dehydroepiandrosterone (DHEA)	53-43-0	288.42
sitosterol	83-46-5	414.71
7α,24(S)-dihydroxycholesterol	245523-67-5	418.65
7α,24(S)-dihydroxy-4-cholesten-3-one	2260669-16-5	416.64
7α-hydroxycholestenone	3862-25-7	400.64
5α-7,24-cholestadiene	651-54-7	384.64
zymostenol	566-97-2	386.65
sitostanol	83-45-4	416.72
cholesteryl phosphocholine (CholPC)	65956-64-1	551.78
N,N-dimethyl-3ß-hydroxycholenamide (DMHCA)	79066-03-8	401.63
campesterol	474-62-4	400.68
7-keto-25-hydroxycholesterol	64907-23-9	416.64
dehydroergosterol (DHE)	516-85-8	394.63
cholestanol	80-97-7	388.67

Sup. Table 1:
List of oxysterols screened against GPR17.

Sup. Figure 1

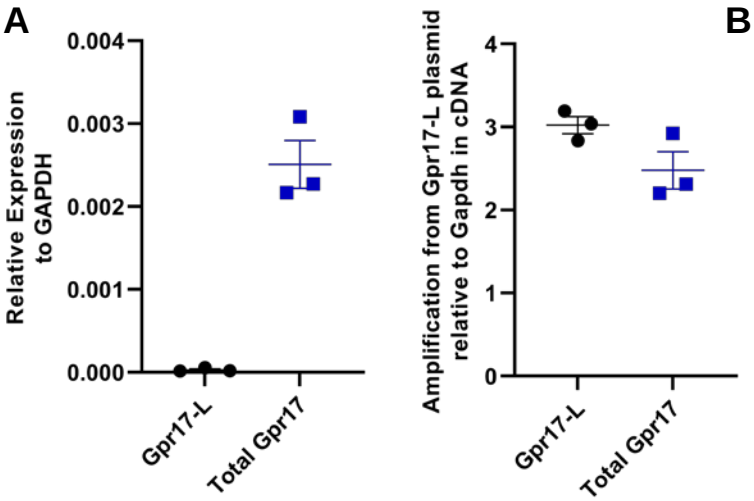

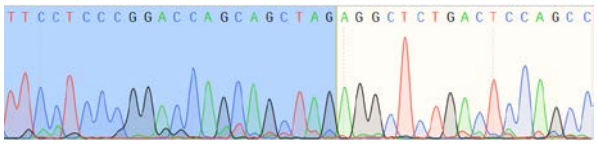

Gpr17 short form sequence, exon 1:
TTCCTCCCGGACCAGCAGCTAGAGGC
TCTGACTCCAGCC

Gpr17 long form sequence, exon 1-2 junction
CAAGAGAGATGCTGAAACTCTCAGGCTCT
GACTCCAGCC

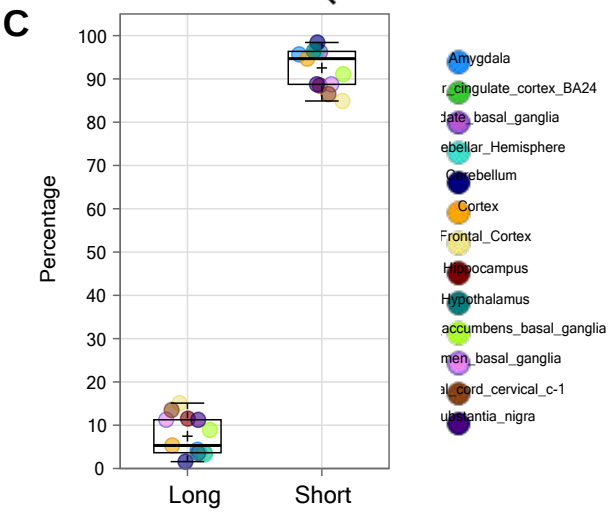

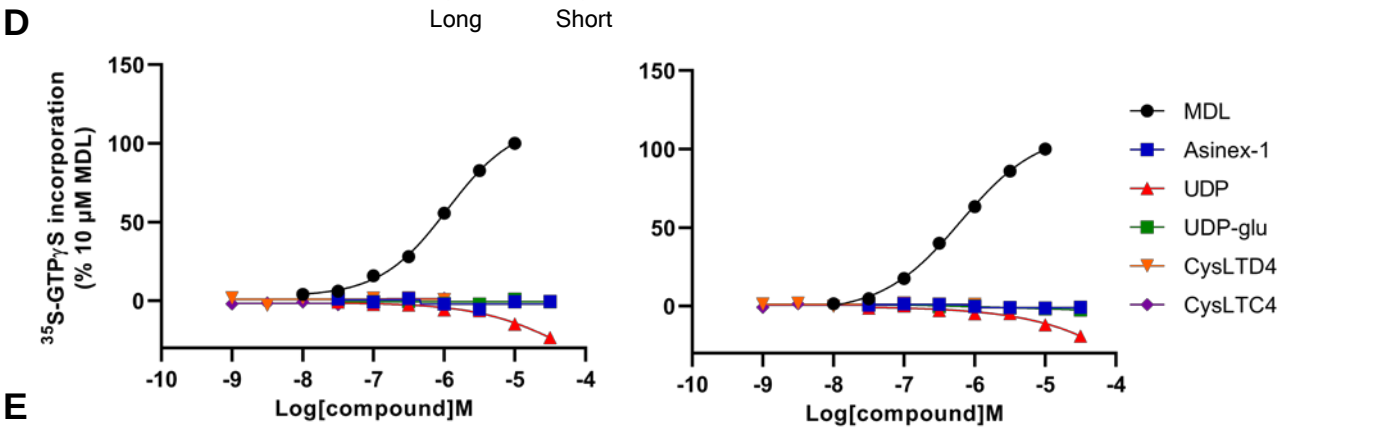

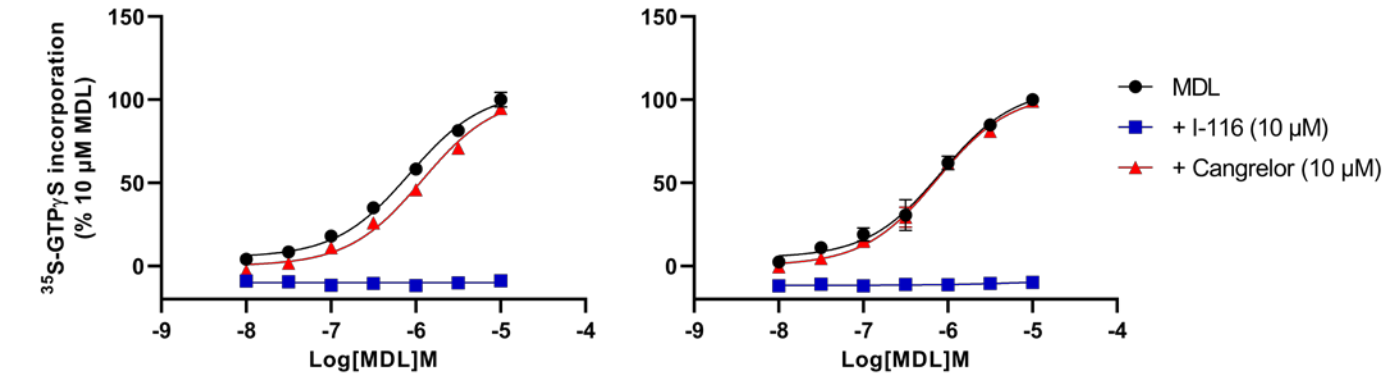

Sup. Figure 1. Quantification of Gpr17 mRNA long and short form expression in human tissues. (A) RT-qPCR analysis of Gpr17 mRNA expression by RT-PCR. GAPDH mRNA was used as the internal control. The results for Gpr17 mRNA expression were normalized versus expression level of GAPDH. Cloned human GPR17 long form was diluted and served as template for PCR to show that the amplification of the long form is equal to the total Gpr17. Assays were performed in triplicates. (**B)** 5' end RACE (rapid amplification of cDNA end) analysis of the human Gpr17 5' end transcription sequences. The 5' end RACE reactions were performed for Gpr17 using human brain RACE ready cDNA (Clontech). The resulting RACE PCR products were sequenced using specific primers for the long and short form respectively or using a common primer. The chromatogram shown above are sequencing results using the common primer but only the short form of Gpr17 mRNA is detected. The experiments were repeated 3 times and identical results were observed. **(C)** RNA-seq analysis for Gpr17 mRNA long and short form expression in the human brains. Proportion of GPR17 long and short isoform expression in human brain areas. **(D)** Pharmacological comparison of Gpr17 long *(left)* and short *(right)* forms using [^{35}S]-GTPγS binding assays. For agonist test, membranes from COS7 cells expressing Gpr17 long and short forms were stimulated with reported Gpr17 agonists including MDL29,951, UDP, UDP-glucose, leukotrienes, and Asinex-1. Experiments were performed in triplicates at each data points. **(E)** For the antagonist test, MDL29,951 was added at 3 uM and I-116 was added to inhibit Gpr17 activation resulting in an IC_{50} of 1.3 nM and 4.1 nM for the long form *(left)* and short form *(right)* respectively. Experiments were performed in triplicates at each data points.

Sup. Figure 2

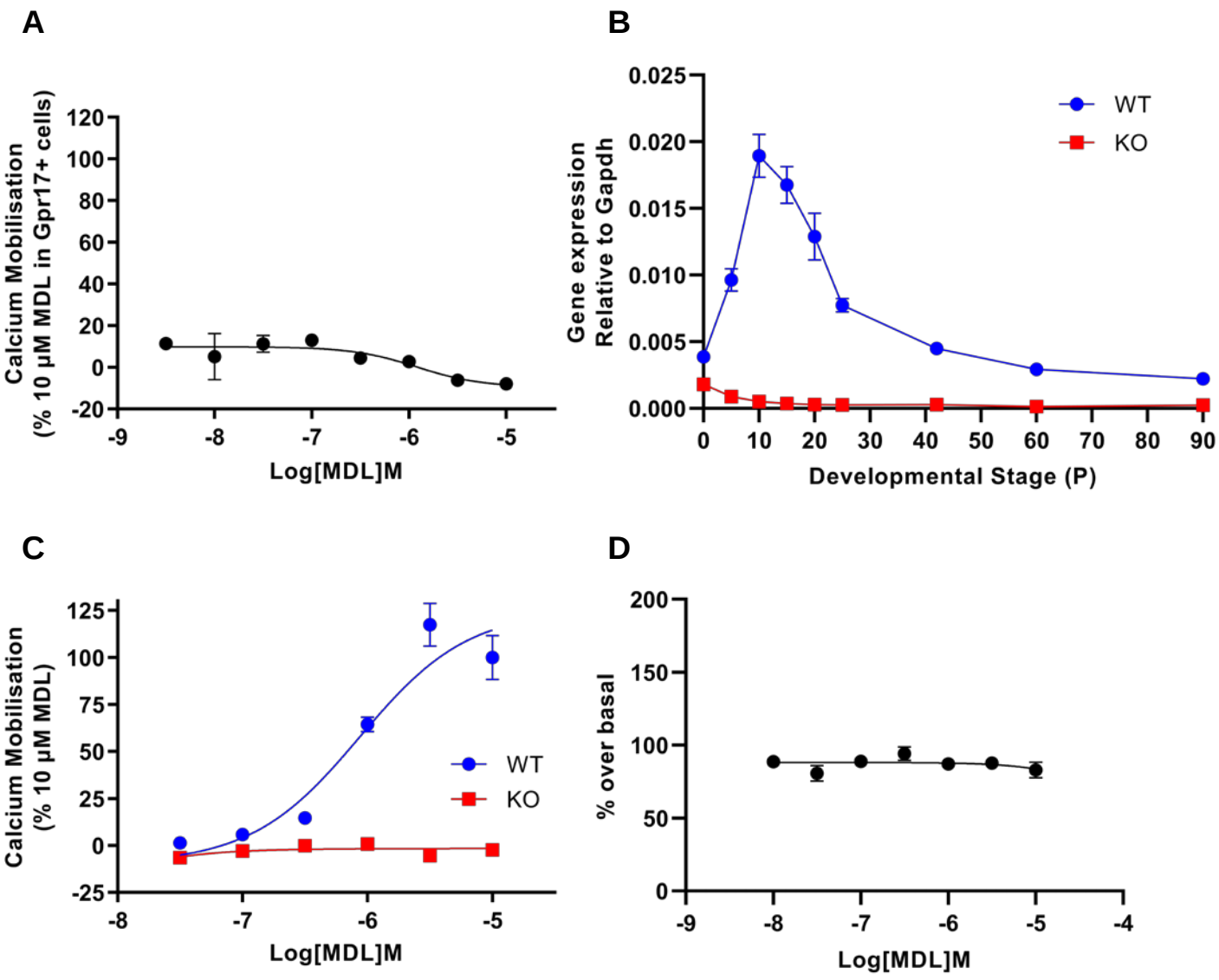

Sup. Figure 2. Specificity of MDL29,951 response for Gpr17. (**A).** Effect of MDL29,951 in control SK-N-MC cells (without Gpr17 expression) in a calcium mobilisation assay using MDL, 29,961 as the ligand. Experiments were performed in triplicates at each data points. (**B**). Gpr17 mRNA expression as measured by RT-PCR in the brains of wild type (WT) and Gpr17 knockout mice. Gpr17 knockout mice were purchased from Deltagen and fully backcrossed with C57/BL6 background mice to congenic. Experiments were performed in triplicates. (**C**). Effect of MDL29,951 on calcium mobilization in OPCs from WT mice and Gpr17 KO mice. Experiments were performed in triplicates at each data points. (**D).** Effects of MDL29,951 on [^{35}S]-GTPγS binding in control COS7 cells (without Gpr17 expression). Experiments were performed in triplicates at each data points.

Sup. Figure 3

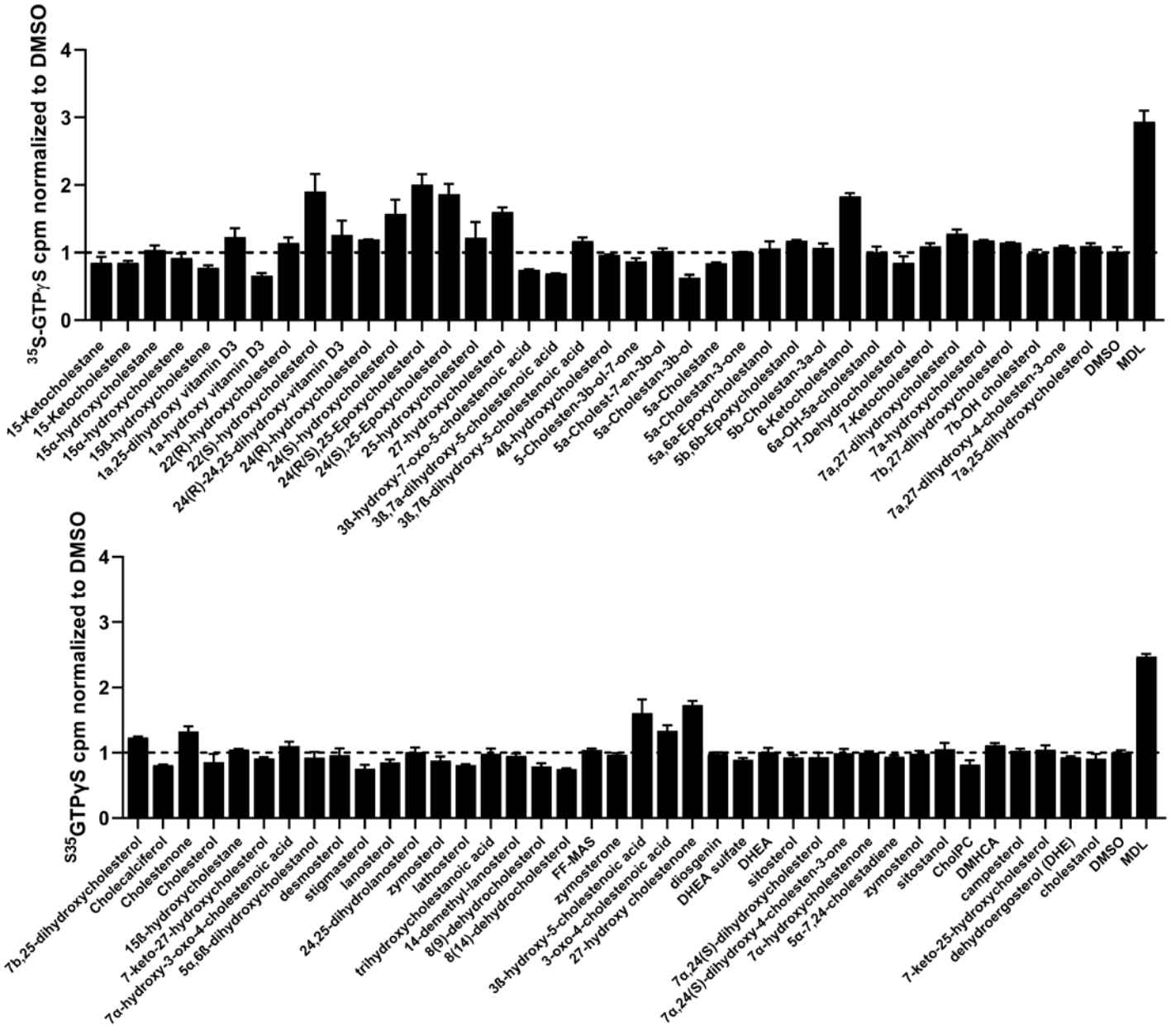

Sup. Figure 3. Screening of oxysterols for activation of Gpr17 using [^{35}S]-GTPγS binding assay. The oxysterols (77) were screened at 10 μM using membranes from COS7 cells co-expressing Gpr17 and Go2 or Go2 alone. Screening assays were performed with duplicates at each data point. MDL29,951 and buffer (DMSO) were used as the positive and negative controls respectively. Results shown are normalized using the results from Go2 control and the result from buffer was set at 100%. Experiment was performed once, with a duplicate at each data point.

Sup. Figure 4

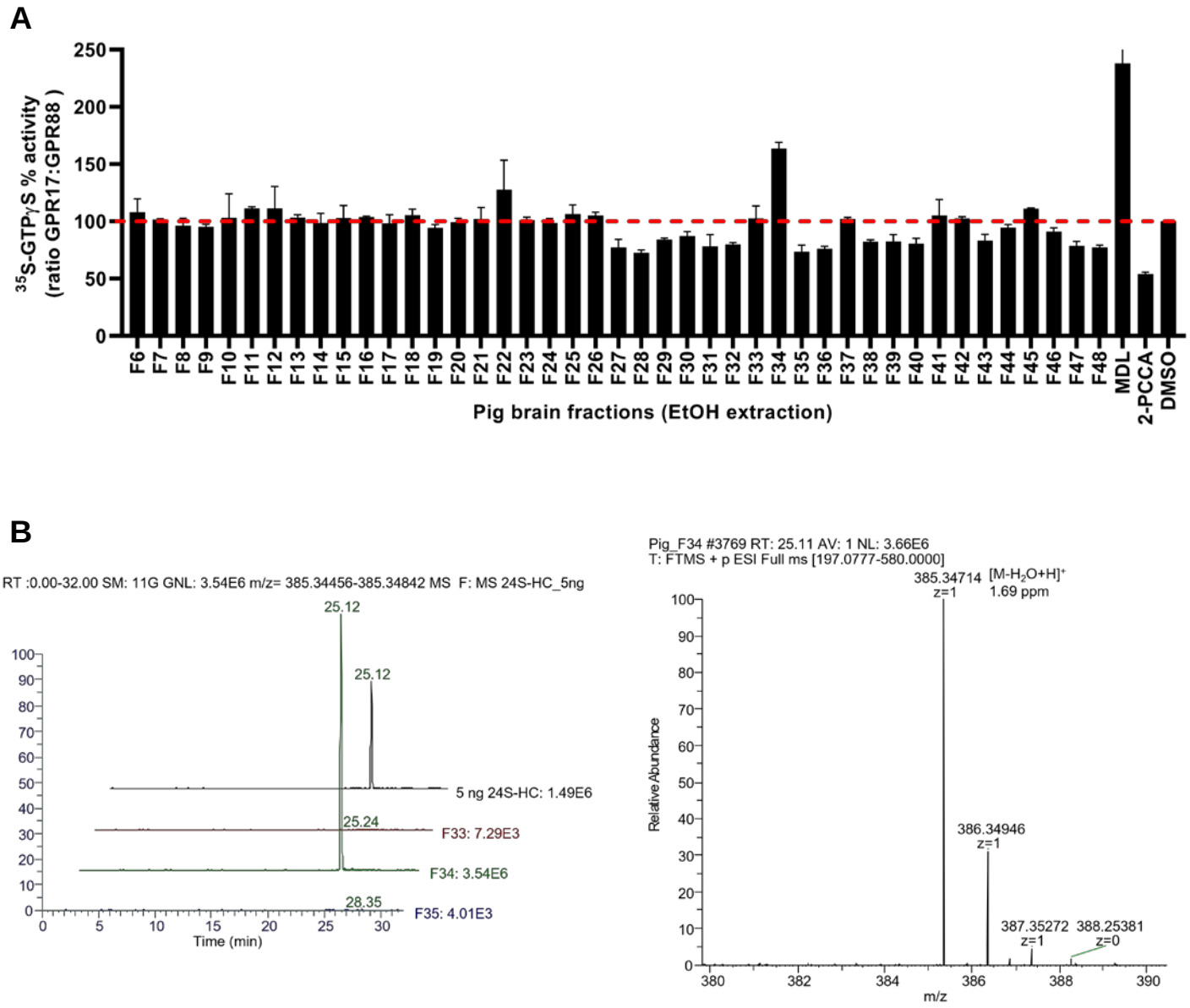

Sup. Figure 4. Pig Brain Fraction: A. Activity for GPR17 activation. B. Extracted ion chromatogram (left). ESI Full MS (right).

Sup. Figure 5

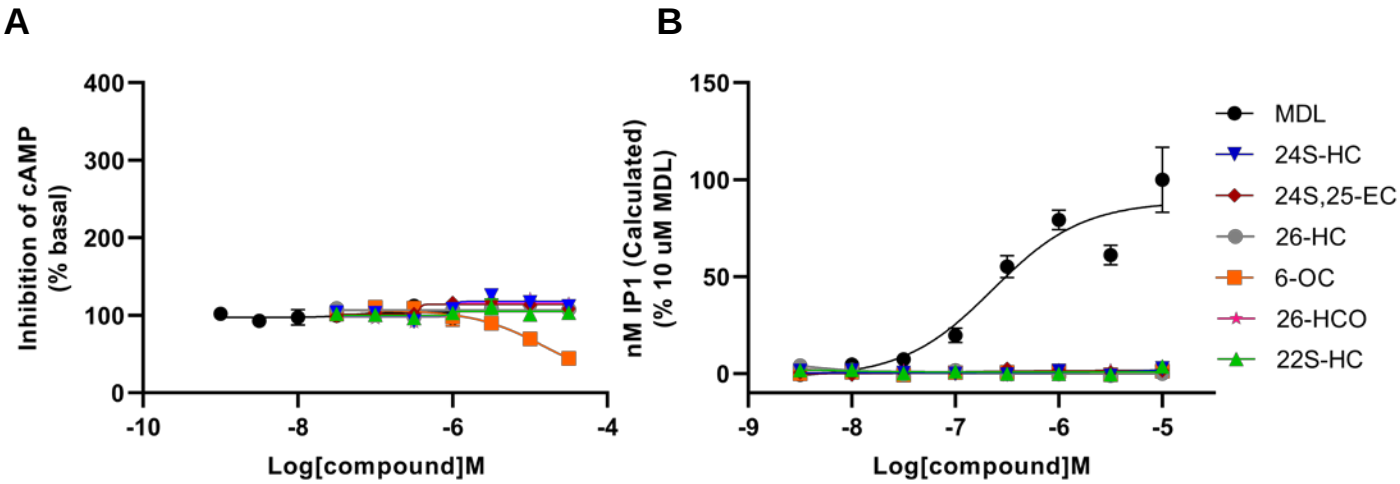

Sup. Figure 5. Specificity of oxysterols as activators of Gpr17 in cAMP and IP1 assays. (**A).** Effects of MDL29,951 and oxysterols on forskolin induced cAMP accumulation in SK-N-MC cells without Gpr17 expression. Experiments were performed in triplicates at each data points. (**B).** Effects of MDL29,951 and oxysterols on IP1 accumulation in Gpr17 expressing SK-N-MC cells. Assays were performed with duplicates at each data point.

Sup. Figure 6

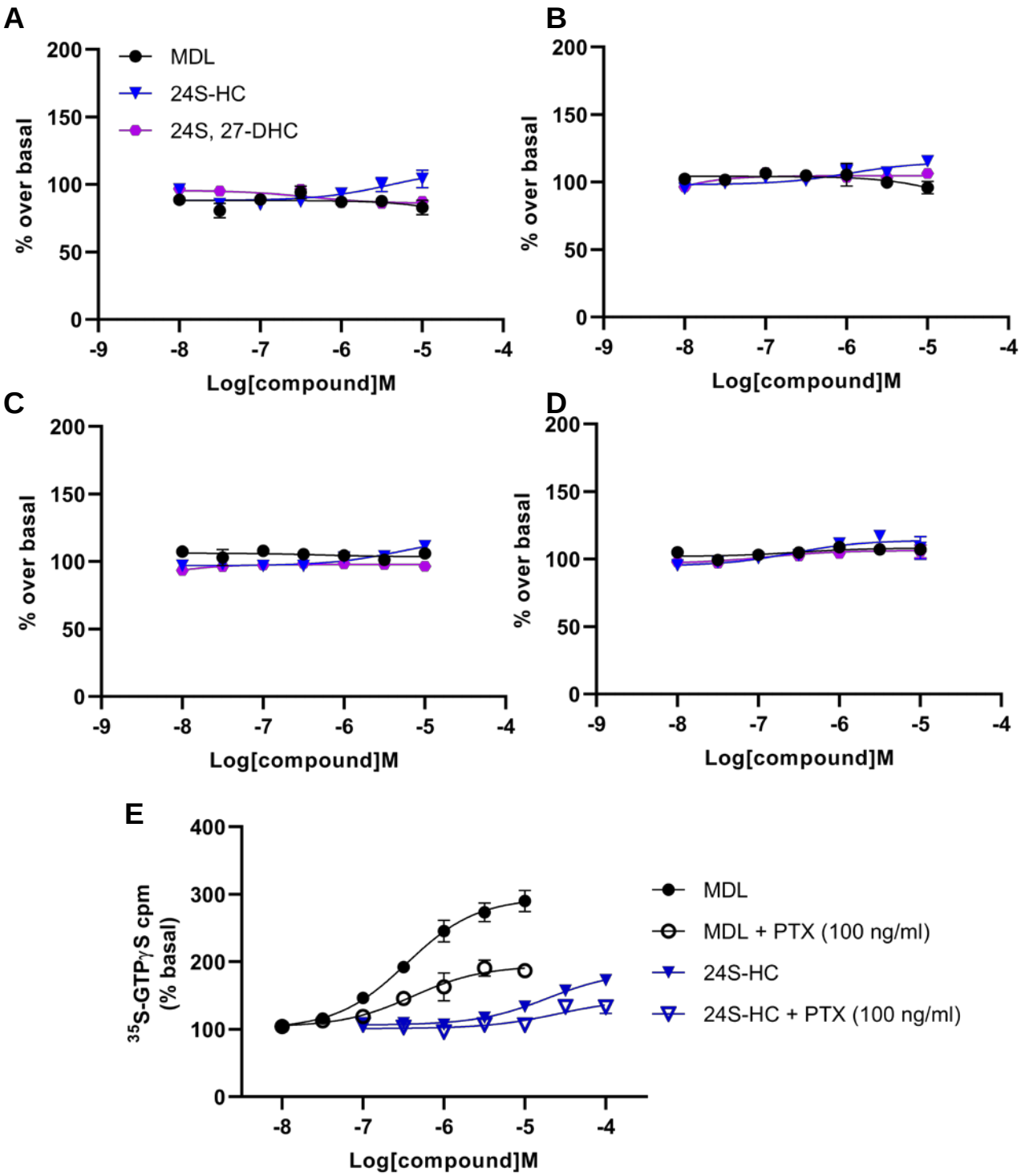

Sup. Figure 6. Characterization of Gpr17 G-protein coupling in [^{35}S]-binding. Concentration response of MDL29,951, 24S-HC and 24S,27-DHC using membrane preparations from COS7 cells with no recombinant protein expression **(A)**, or specific expression of Go2 **(B)**, Go2q **(C)**, Go2s **(D)**. **(E).** Concentration response of MDL29,951 and 24S-HC in GTPγS binding assays using pertussis-toxin (100 ng/ml) treated or non-treated membrane preparations from COS-7 cells co-expressing Gpr17 and Go2. Data is expressed as percent of basal response (buffer). Experiments were performed in triplicates at each data points.

Sup. Figure 7

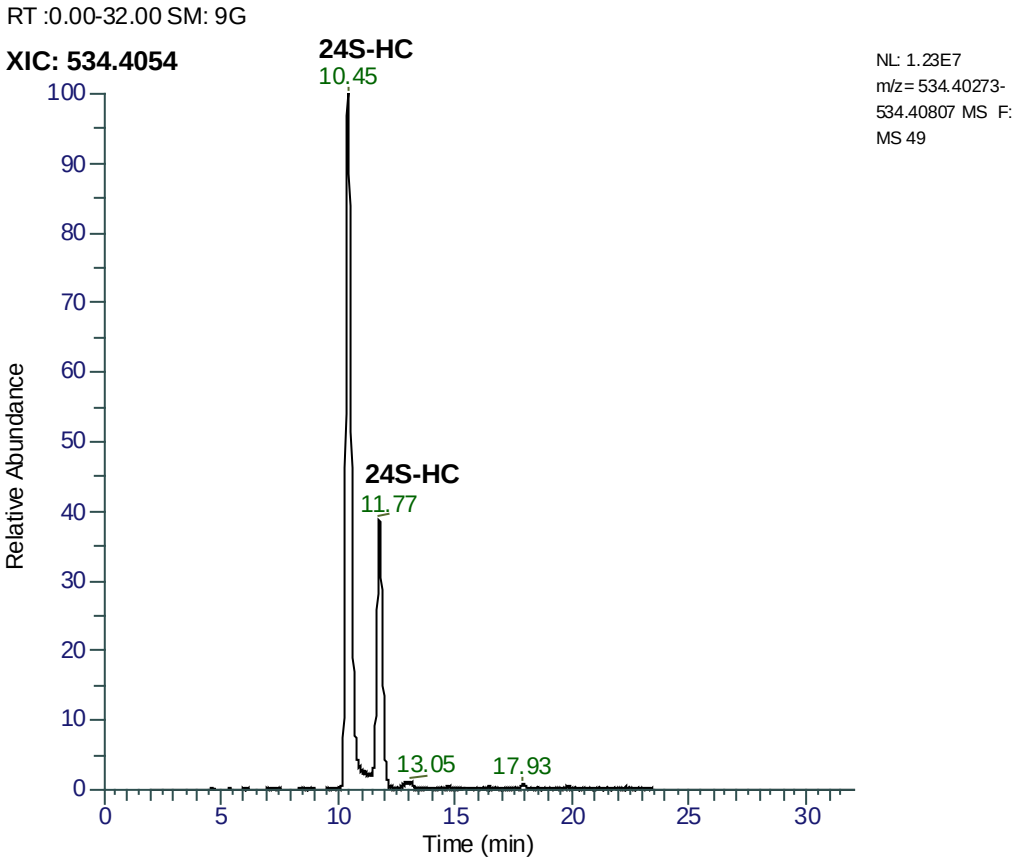

Sup. Figure 7. Relative abundance of 24S-HC to other oxysterols in mouse brain. **The main two peaks represent signals from 24S-HC. Other oxysterols are just at or below the detection margin.** Experiments were performed in quadruplicates (n = 4) and representative graph is shown. 24S-HC is verified by its molecular weight, retention time, and substructures determined by mass-2 analysis.